

Local measurement of the Eliashberg function of Pb islands: enhancement of electron-phonon coupling by quantum well states

Michael Schackert,¹ Tobias Märkl,¹ Jasmin Jandke,¹ Martin Hölzer,² Sergey Ostanin,² Eberhard K. U. Gross,² Arthur Ernst,^{2,3} and Wulf Wulfhekel¹

¹*Physikalisches Institut, Karlsruhe Institute of Technology,
Wolfgang-Gaede-Straße 1, 76131 Karlsruhe, Germany*

²*Max-Planck Institut für Mikrostrukturphysik, Weinberg 2, 06120 Halle, Germany*

³*Wilhelm-Ostwald-Institut für Physikalische und Theoretische Chemie,
Linnéstraße 2, Universität Leipzig, 04103 Leipzig, Germany*

(Dated: September 30, 2018)

Inelastic tunneling spectroscopy of Pb islands on Cu(111) obtained by scanning tunneling microscopy below 1 K provides a direct access to the local Eliashberg function of the islands with high energy resolution. The Eliashberg function describes the electron-phonon interaction causing conventional superconductivity. The measured Eliashberg function strongly depends on the local thickness of the Pb nanostructures and shows a sharp maximum when quantum well states of the Pb islands come close to the Fermi energy. *Ab initio* calculations reveal that this is related to enhanced electron-phonon coupling at these thicknesses.

PACS numbers: 74.25.Kc, 74.25.Jb, 73.21.-b

In conventional superconductors (SC) Cooper pairs are formed due to electron-electron interaction via virtual phonon exchange. While this concept already lies at the heart of the BCS theory [1] it turned out soon that the simplifications by the assumptions of the BCS theory are too crude. Especially when dealing with so-called strong coupling SCs an extension of the theory is required which was presented by Eliashberg [2]. He took into account that the electron-phonon interaction is local in space and retarded in time. A central quantity in this theory is the effective electron-phonon spectrum $\alpha^2 F(\omega)$, which is also called Eliashberg function. Here $F(\omega)$ is the phonon density of states (DOS) and α (which actually is $\alpha(\omega)$), is the energy dependent electron-phonon coupling strength. The Eliashberg theory allows to calculate the properties for all conventional SCs once $\alpha^2 F(\omega)$ is known.

While the experimental determination of $F(\omega)$ can be achieved by inelastic neutron scattering, this technique provides no immediate access to the full Eliashberg function since it contains the electron-phonon coupling strength, which is not directly accessible with neutrons. On the other hand it was shown that the Eliashberg function can be calculated from the quasiparticle DOS of a SC extracted from tunneling experiments by inverting the Eliashberg gap equations [3]. Although this method could confirm the validity of the Eliashberg theory it is a rather indirect way of obtaining $\alpha^2 F(\omega)$. Especially in the case of multiple superconducting gaps, the inversion is not unique.

Inelastic tunneling spectroscopy (ITS), however, provides a direct access to the excitations in a solid. Using scanning tunneling microscopy (STM), in addition, offers the possibility of performing ITS with high spatial resolution [4]. Most STM-ITS experiments were dedicated to molecular vibrations but there are, though rarely, studies

of collective vibrations as well [5]. The principle of ITS is based on the opening of an inelastic tunneling channel in parallel to the elastic one as soon as the energy of the tunneling electrons overcomes the threshold for performing an excitation in the sample leading to an increase of the differential conductivity dI/dU . Since the latter is only of a few percent it is common to use a lock-in amplifier and record the second derivative of the tunneling current with respect to the bias voltage, $d^2 I/dU^2$, which reveals a peak at the positive voltage corresponding to the energy of the excitation. Due to the symmetry of electron and hole tunneling, a minimum (dip) is found at the same voltage on the negative bias side. A dip-peak pair is thus a characteristic fingerprint of an inelastic tunneling process. So far, we only considered excitations at discrete energies. In systems possessing a continuous spectrum of excitations, as in the case of phonons, the second derivative of the tunneling current is proportional to their DOS $F(\omega)$:

$$\left. \frac{d^2 I}{dU^2} \right|_{U=\hbar\omega/e} \propto \rho_t(E_F) \rho_s(E_F) F(\omega) |M_{inel}(eU)|^2. \quad (1)$$

Here $\rho_t(E_F)$ and $\rho_s(E_F)$ are the electronic DOS of the tip and the sample, respectively, and are taken to be constant around E_F . $M_{inel}(eU)$ is the matrix element for inelastic tunneling which, in the case of phonons, is proportional to the electron-phonon coupling strength α due to the optical theorem [6]. In a SC, however, the formation of the gap below the superconducting transition temperature (T_c) leads to a strong energy dependence of $\rho_s(E)$. Since the conductance of a tunnel junction is directly proportional to the electronic DOS, the gap feature dominates the signal in $d^2 I/dU^2$. For this reason, superconductivity has to be suppressed. In principle, there are two possibilities to force a SC into its normal state even

below T_c . One is to apply a magnetic field, the other one is to use the proximity effect of a SC in contact with a normal metal.

In this Letter, we report on the first direct and spatially resolved study of the Eliashberg function by STM. We used Pb islands on Cu(111) as a model system for this novel approach and find strong dependencies of the Eliashberg function on the local electronic properties.

Pb belongs to the so-called strong coupling SCs. The value of $2\Delta_0/k_B T_c = 4.4$ lies far above the BCS value of 3.52 and it is the material with the strongest electron-phonon coupling among the elemental SCs [7] and has therefore been widely studied in the past. Pb was among the systems which were investigated in the pioneering work of Giaever *et al.* who were able to obtain the quasi-particle DOS from planar tunnel junctions [8]. Indeed, it was this measurement from which the Eliashberg function of a SC was obtained for the first time using the McMillan gap inversion method [3]. The Eliashberg function of Pb exhibits two prominent maxima at around 4 meV and 8 meV. By regarding the phonon dispersion relation these features can be ascribed to van Hove singularities of the transverse and longitudinal phonon modes, respectively [9–11].

In recent years, especially thin Pb islands attracted much attention since the vertical confinement of the electrons results in discrete quantum well states (QWS), which were found to have a substantial influence on the growth mode [12, 13]. When Pb is deposited onto Cu(111) at room temperature (RT), the growth mode is of Stranski-Krastanov type [14], i. e. islands start to grow once a wetting layer is complete. These islands are (111)-oriented nanocrystallites with a height distribution that is not statistical. Instead, as was first observed by Otero *et al.*, certain "magic" heights are strongly preferred while some other numbers of monolayers (ML) seem to be "forbidden" [15]. The authors show that the appearance of these preferred heights is directly correlated to the QWS. A thickness for which a QWS is near the Fermi level is energetically unfavored and thus, when growing, the system avoids those numbers of ML. Moreover, an influence of the QWS on the electron-phonon coupling and on T_c has been demonstrated for Pb films on semiconducting Si(111)-(7 × 7) [16–18]. Different results were published, in which T_c rises [16, 17] or slightly falls [18] with the film thickness superimposed with weak oscillations. In contrast, Pb islands on Cu(111) are expected to be in the normal due to the proximity effect of the metallic substrate [19]. Hence, Pb/Cu(111) should provide an ideal system to study the phonon excitations by STM-ITS in the normal state and to resolve the details of the influence of the QWS on the Eliashberg function as well.

The preparation and study of the sample were carried out in UHV ($p \approx 10^{-10}$ mbar) in a home-made low temperature STM setup [20]. In particular, this setup com-

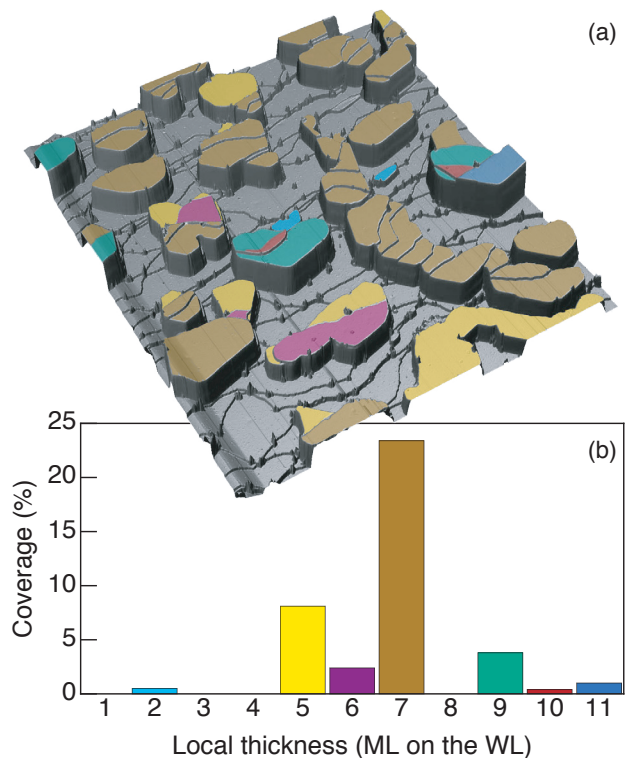


FIG. 1: (a) STM topography ($800 \times 800 \text{ nm}^2$, 1 V, 100 pA) showing Pb islands on the stepped Cu(111) surface. The colored surfaces indicate the local thickness whose distribution is given in (b).

prises a Joule-Thomson refrigerator operated with a ^3He - ^4He mixture which allows for a base temperature below 700 mK. The Cu(111) single crystal was cleaned by sputtering with Ar^+ ions at 1.5 kV and subsequent annealing at 500 °C. After the sample had cooled down to RT, Pb was evaporated by electron bombardment and a total amount of 3.8 ML was deposited at a rate of 1.9 ML/min. An electrochemically etched W wire, which was treated by several cycles of Ar^+ sputtering and flash-annealing, was used as STM tip. The temperature of the sample and the tip was (0.8 ± 0.1) K during the measurements. For ITS the tip was stabilized at 20 mV and 50 nA and the spectra were obtained by measuring the second derivative of the tunneling current using lock-in technique [21] with a modulation voltage of 400 μV (RMS) at a frequency of 16.2 kHz. Recording a single spectrum was set to take 3 min but in order to increase the signal-to-noise ratio 20 spectra were taken successively at the same point and averaged to one spectrum. These spectra are shown without any subsequent filtering.

Fig. 1(a) shows a typical STM topography of the sample. Pb islands of a lateral size of about 100 nm grow on top of the wetting layer on the stepped Cu(111) surface. Most of the islands span one or more Cu steps and many of them coalesce. In order to determine the local thickness we considered the height profiles extracted from the

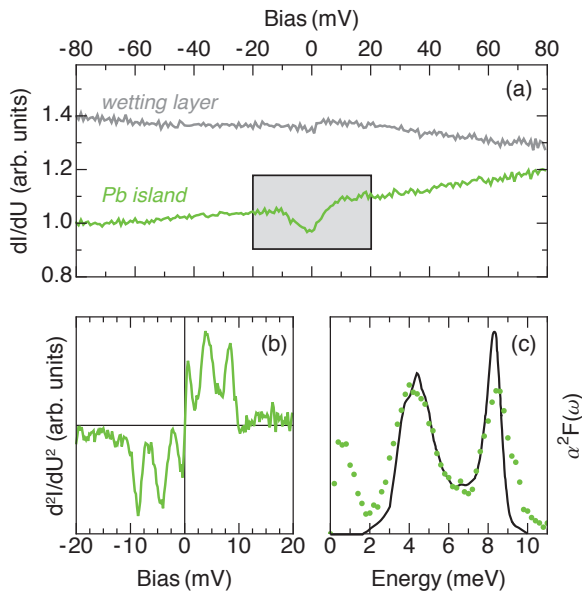


FIG. 2: (a) Large energy range tunneling conductance spectra (normalized and shifted) of the wetting layer and of a 12 ML thick Pb area. While the conductance of the wetting layer is constant, the Pb island exhibits a significant decrease of conductance at zero bias. The perfect antisymmetric shape of the d^2I/dU^2 spectrum (b) taken on the same position in a smaller bias interval around E_F doubtlessly reveals the origin of the reduced conductance being an inelastic process. (c) Average of the positive and negative bias side of the ITS spectrum in (b) (dots) in comparison with the previous result for $\alpha^2F(\omega)$ (line) [3].

STM topography as well as the QWS [15]. In Fig. 1(a) the Pb areas are marked with different colors according to their local thickness whereas Fig. 1(b) shows the thickness distribution. Most of the islands have a constant thickness of 5 or 7 ML on top of the wetting layer, which are thus the "magic heights" for this amount of Pb. As can be seen in Fig. 1(a) and 3(a), there are, however, some islands which change their thickness by 1 or 2 ML when growing over a Cu step edge and closely spaced steps may even help to stabilize unfavored heights, as was already observed before [15]. In particular, there are only two rather small regions in Fig. 1(a) that are 10 ML thick and 8 ML was not observed at all.

We performed dI/dU spectroscopy on the Pb regions of different heights as well as on the wetting layer. In Fig. 2 we show exemplarily the results for a Pb thickness of 12 ML. In contrast to the constant differential conductance of the wetting layer there is a pronounced dip around E_F in the case of Pb islands. The same effect was observed for Pb islands on Si(111)-(7 × 7) [22, 23]. Since the experiment of Wang *et al.* was performed at 10 K, which is above T_c of Pb, the authors termed this feature "pseudo gap" as in the field of high temperature superconductivity. We, however, attribute the dip to inelastic

excitations. We present a high resolution d^2I/dU^2 spectrum of this energy range in Fig. 2(b). An almost point-symmetric shape is obtained showing two dominant dip-peak pairs at a bias of about ± 4.0 mV and ± 8.3 mV as well as one very close to zero bias (± 0.6 mV). A comparison to the previously determined Eliashberg function of Pb [3] is provided in Fig. 2(c) and since it reveals an almost perfect agreement there is strong evidence that the ITS data directly yields the Eliashberg function. i. e. the dip does not indicate a pseudo gap. Only the feature closest to E_F is not related to $\alpha^2F(\omega)$ but is due to a zero bias anomaly (ZBA), as already observed in planar tunneling experiments on Pb [24].

After confirming that STM-ITS is able to measure the Eliashberg function we focussed on the thickness dependence. In particular, we investigated a "wedge"-like island (Fig. 3(a)) the height of which increases by 1 ML at every underlying step starting from 10 ML. Keeping all parameters constant, we recorded d^2I/dU^2 spectra (Fig. 3(d)) on every local thickness and we were able to find the ZBA and the Eliashberg function in all cases. While the former stays the same there is a strong thickness dependence of the intensity of $\alpha^2F(\omega)$. For areas comprising an odd number of ML it is relatively weak whereas the signal gets stronger for 12 ML and is by far strongest for 10 ML as can also be seen in the d^2I/dU^2 map, i. e. a map of the local electron-phonon coupling at 8 meV, in Fig. 3(c) recorded with the bias set to the energy of the longitudinal peak. No differences were found for different locations within an area of a given thickness. Note that in all experiments, the current was set to the same value during tip stabilization, such that the differ-

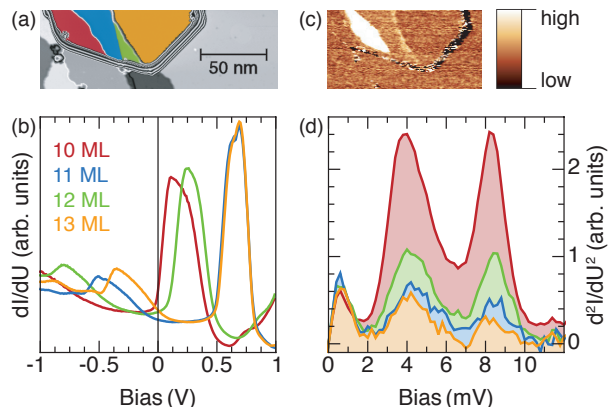


FIG. 3: (a) Topographic image of a wedge shaped island. The color code of the Pb areas corresponds to the thicknesses given in (b) where the QWS obtained from the dI/dU spectra at an arbitrary location on the Pb areas of different heights are shown. (d) Average of the positive and negative bias side of the ITS spectra recorded at the same locations as in (b). The intensity of the $\alpha^2F(\omega)$ increases considerably on the 10 ML high Pb area as can also be seen from the d^2I/dU^2 map of the same island taken at 8 mV (c).

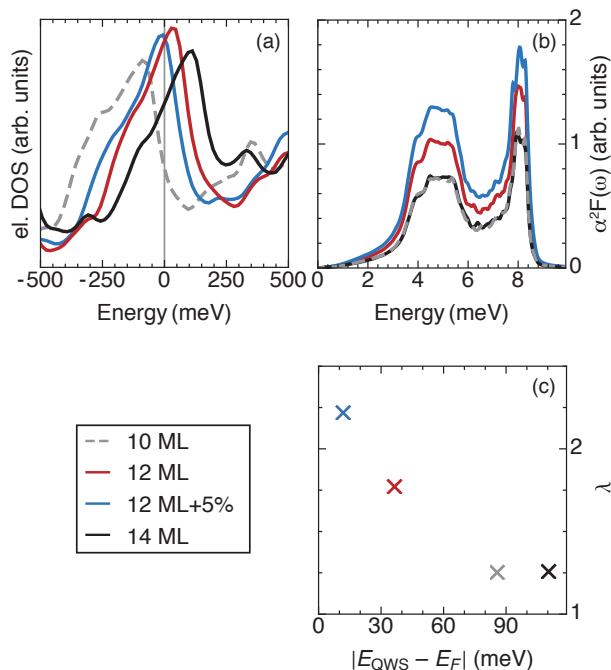


FIG. 4: Theoretical calculation. (a) QWS in the electronic DOS (at the first vacuum layer). (b) Eliashberg function. (c) Resulting electron-phonon coupling constant λ .

ences in the inelastic spectra are not related to differences in the electronic DOS. Since we expected that the thickness dependence should be influenced by the electronic QWS, we measured the first derivative of the tunneling current in a larger voltage range (Fig. 3(b)). In the case of the odd numbers of ML, the highest occupied as well as the lowest unoccupied states lie roughly 0.5 eV away from the Fermi level. In contrast, the lowest unoccupied QWS of the 10 ML and 12 ML thick layers are very close to E_F . The relevant QWS of the former, which exhibited also the highest $\alpha^2 F(\omega)$ intensity, is closest to E_F . Thus, our experiment clearly shows, that electron-phonon coupling can be strongly enhanced (factor 5), if unoccupied QWS are near the Fermi energy.

To elucidate the experimental finding, we calculated the electronic structure and phonons for different free standing Pb films. The structural relaxations and the phonons were computed using the VASP code, well known for precise total energy and forces calculations [25], while the electronic structure of the thin films was obtained with a first-principles Green's function method, specially designed for semi-infinite systems such as surfaces and interfaces [26]. The self-consistently calculated Green's functions and phonons were used to compute the Eliashberg function of the given systems.

First of all, we found QWS in this systems in qualitative agreement with the experiment. The calculated electronic DOS exhibits a QWS closest to the Fermi level

for a thickness of 12 ML while for 10 ML and 14 ML the QWS lie roughly 0.1 eV below and above E_F , respectively (Fig. 4(a)). The theoretical results for $\alpha^2 F(\omega)$ in Fig. 4(b) reveal the same effect as the experiment. While the intensity of $\alpha^2 F(\omega)$ is the same for 10 and 14 ML, it increases by more than 30 % in the case of 12 ML. Also shown in Fig. 4 is the effect of compressing the surface of the 12 ML slab by 5%. This compression shifts the QWS even closer to E_F which again is accompanied by a further increase of the intensity of $\alpha^2 F(\omega)$. Fig. 4(c) comprises the resulting electron-phonon coupling constant λ , which changes from a value of about 1.25 to 2.2, i.e. significantly above the bulk value, upon the shift of the QWS towards E_F . Thus, in qualitative agreement to the experiment, the Eliashberg function can be increased by a QWS near the Fermi level. Quantitatively, the experimental enhancement of the electron-phonon coupling is even stronger than theoretically predicted by a factor of 2-3, possibly due to the details of the quantum well states of Pb on Cu(111).

The mechanism leading to the enhancement can be understood from total energy considerations. The formation of QWS in thin Pb films leads to an energetically unfavourable condition when a QWS lies very close to E_F . A change of the lattice constant, e.g. by a phonon, shifts the QWS up and down through the Fermi level and leading to repopulation of the electrons with large changes of the electronic energy. Thus, deformations couple more strongly to the electronic degrees of freedom when a QWS is near the Fermi energy increasing the electron-phonon coupling. Supposed that the behavior is similar on Si(111), our findings could also explain the T_c oscillation with the thickness as it was observed in that system [18].

In conclusion, we demonstrated that, using low temperature STM-IST, it is possible to directly measure phonon excitations in Pb islands. The obtained $d^2 I/dU^2$ spectra can be unambiguously identified as $\alpha^2 F(\omega)$ which allows for the experimental determination of the latter with the high spatial resolution of the STM. We found a pronounced dependence of the Eliashberg function on the thickness of the Pb slabs which, with the aid of *ab initio* calculations, can be explained by their energetic stability due to the position of the electronic QWS. This mechanism, if generally applicable, can be used to increase T_c of conventional superconductors by using layered structures with QWS at appropriate energies.

M.S. acknowledges funding by the Karlsruhe House of Young Scientists (KHYS).

-
- [1] J. Bardeen, L. N. Cooper, and J. R. Schrieffer, Phys. Rev. **108**, 1175 (1957).
 [2] G. Eliashberg, Soviet Physics **11**, 696 (1960).

- [3] W. L. McMillan and J. M. Rowell, Phys. Rev. Lett. **14**, 108 (1965).
- [4] B. C. Stipe, M. A. Rezaei, and W. Ho, Science **280**, 1732 (1998).
- [5] L. Vitali, M. A. Schneider, K. Kern, L. Wirtz, and A. Rubio, Phys. Rev. B **69**, 121414 (2004).
- [6] C. Cohen-Tannouji, F. Diu, and F. Laloe, *Quantenmechanik 2* (de Gruyter, 2010).
- [7] W. Buckel, *Supraleitung: Grundlagen und Anwendungen* (Wiley, 2004).
- [8] I. Giaever, H. R. Hart, and K. Megerle, Phys. Rev. **126**, 941 (1962).
- [9] R. Heid, K.-P. Bohnen, I. Y. Sklyadneva, and E. V. Chulkov, Phys. Rev. B **81**, 174527 (2010).
- [10] B. N. Brockhouse, T. Arase, G. Caglioti, K. R. Rao, and A. D. B. Woods, Phys. Rev. **128**, 1099 (1962).
- [11] R. Stedman, L. Almqvist, and G. Nilsson, Phys. Rev. **162**, 549 (1967).
- [12] R. Otero, A. L. Vázquez de Parga, and R. Miranda, Surface Science **447**, 143 (2000).
- [13] W. B. Su, S. H. Chang, W. B. Jian, C. S. Chang, L. J. Chen, and T. T. Tsong, Phys. Rev. Lett. **86**, 5116 (2001).
- [14] J. Camarero, J. Ferrón, V. Cros, L. Gómez, A. L. Vázquez de Parga, J. M. Gallego, J. E. Prieto, J. J. de Miguel, and R. Miranda, Phys. Rev. Lett. **81**, 850 (1998).
- [15] R. Otero, A. L. Vázquez de Parga, and R. Miranda, Phys. Rev. B **66**, 115401 (2002).
- [16] Y.-F. Zhang, J.-F. Jia, T.-Z. Han, Z. Tang, Q.-T. Shen, Y. Guo, Z. Q. Qiu, and Q.-K. Xue, Phys. Rev. Lett. **95**, 096802 (2005).
- [17] Y. Guo, Y.-F. Zhang, X.-Y. Bao, T.-Z. Han, Z. Tang, L.-X. Zhang, W.-G. Zhu, E. G. Wang, Q. Niu, Z. Q. Qiu, et al., Science **306**, 1915 (2004).
- [18] D. Eom, S. Qin, M.-Y. Chou, and C. K. Shih, Phys. Rev. Lett. **96**, 027005 (2006).
- [19] P. Hilsch, Z. Physik **167**, 511 (1962).
- [20] L. Zhang, T. Miyamachi, T. Tomanić, R. Dehm, and W. Wulfhekel, Review of Scientific Instruments **82**, 103702 (2011).
- [21] B. C. Stipe, M. A. Rezaei, and W. Ho, Phys. Rev. Lett. **82**, 1724 (1999).
- [22] T. Nishio, T. An, A. Nomura, K. Miyachi, T. Eguchi, H. Sakata, S. Lin, N. Hayashi, N. Nakai, M. Machida, et al., Phys. Rev. Lett. **101**, 167001 (2008).
- [23] K. Wang, X. Zhang, M. M. T. Loy, T.-C. Chiang, and X. Xiao, Phys. Rev. Lett. **102**, 076801 (2009).
- [24] W. Wattamaniuk, H. Kruezer, and J. Adler, Physics Letters A **37**, 7 (1971).
- [25] G. Kresse and J. Furthmüller, Phys. Rev. B **54**, 11169 (1996).
- [26] M. Lüders, A. Ernst, W. M. Temmerman, Z. Szotek, and P. J. Durham, J. Phys.: Condens. Matter **13**, 8587 (2001).